

Design, Synthesis, and Structural and Spectroscopic Studies of Push–Pull Two-Photon Absorbing Chromophores with Acceptor Groups of Varying Strength

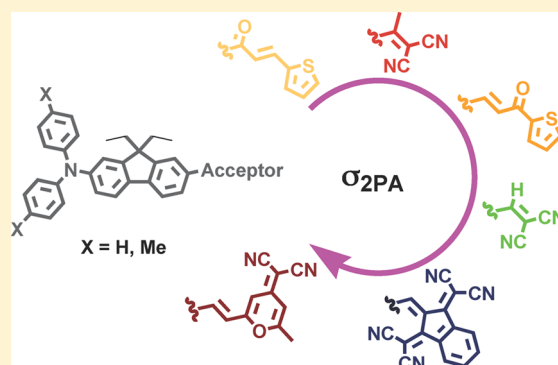
Alma R. Morales,[†] Andrew Frazer,[†] Adam W. Woodward,[†] Hyo-Yang Ahn-White,[†] Alexandr Fonari,[§] Paul Tongwa,[§] Tatiana Timofeeva,[§] and Kevin D. Belfield^{*,†,‡}

[†]Department of Chemistry and [‡]CREOL, The College of Optics and Photonics, University of Central Florida, Orlando, Florida 32816-2366, United States

[§]Department of Biology and Chemistry, New Mexico Highlands University, Las Vegas, New Mexico 87701, United States

Supporting Information

ABSTRACT: A new series of unsymmetrical diphenylaminofluorene-based chromophores with various strong π -electron acceptors were synthesized and fully characterized. The systematic alteration of the structural design facilitated the investigation of effects such as molecular symmetry and strength of electron-donating and/or -withdrawing termini have on optical nonlinearity. In order to determine the electronic and geometrical properties of the novel compounds, a thorough investigation was carried out by a combination of linear and nonlinear spectroscopic techniques, single-crystal X-ray diffraction, and quantum chemical calculations. Finally, on the basis of two-photon absorption (2PA) cross sections, the general trend for π -electron accepting ability, i.e., ability to accept charge transfer from diphenylamine was: 2-pyran-4-ylidene malononitrile (pyranone) > dicyanovinyl > bis(dicyanomethylidene)indane > 1-(thiophen-2-yl)propenone > dicyanoethylenyl > 3-(thiophen-2-yl)propenone. An analogue with the 2-pyran-4-ylidene malononitrile acceptor group exhibited a nearly 3-fold enhancement of the 2PA cross section (1650 GM at 840 nm), relative to other members of the series.



INTRODUCTION

Conjugated organic molecules with large delocalized π -electron systems continue to be the subject of very active research due to their potential use in nonlinear optics and emerging photonics technologies. Generally, such molecules provide substantial delocalization of π -electrons over the molecule, enhancing polarizability and nonlinear optical properties. Among the various classes of nonlinear optical materials, multiphoton absorbing materials continue to attract increasing interest. Two-photon absorption (2PA) is a nonlinear process that involves the somewhat unusual capability of a molecule to absorb two photons simultaneously in order to populate an energy level within the molecule with energy equal to the sum of the energies of the two photons absorbed.¹ 2PA-based chromophores are of particular interest because of their utility and potential in numerous applications such as fluorescence bioimaging,^{2–9} two-photon power-limiting devices,^{10–12} and two-photon photodynamic therapy.^{13–15}

Dipolar push–pull chromophores perhaps constitute the vast majority of compounds investigated for their nonlinear optical properties.^{16–20} Push–pull chromophores involve electron-donor and electron-acceptor groups interacting through a π -conjugating spacer. It has been well-established that modulating the degree of ground-state polarization, or the degree of charge

separation in the ground state of these molecules, can exert significant influence over their molecular polarizability and hyperpolarizabilities.^{21,22} This charge separation in the ground state can be controlled primarily by either modifying the chemical structure, i.e., altering the strength of the donating and accepting substituents, and/or by extending the π -conjugated path.¹⁸ The effects of altering the chemical structure in this way were detailed by Oudar in 1977.²³

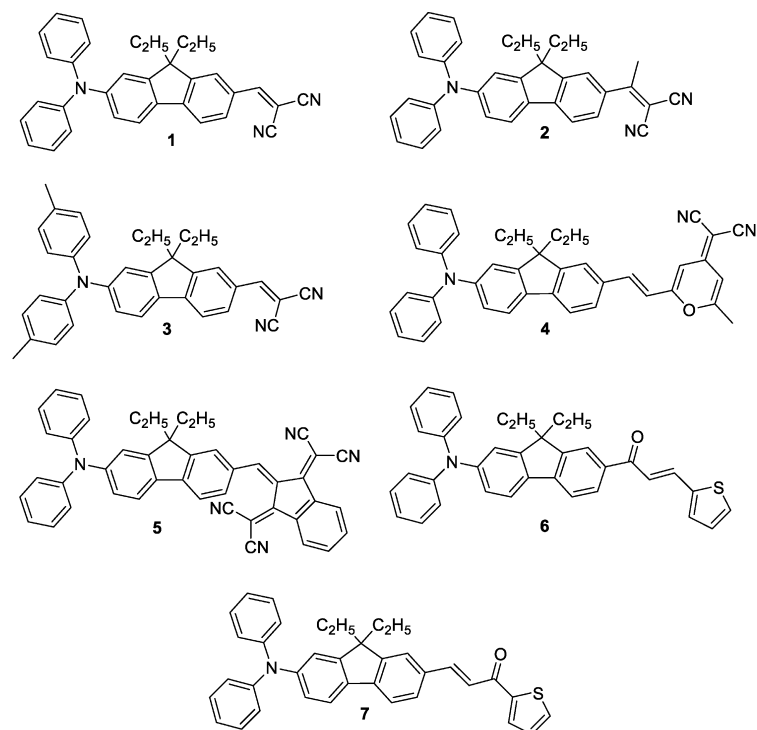
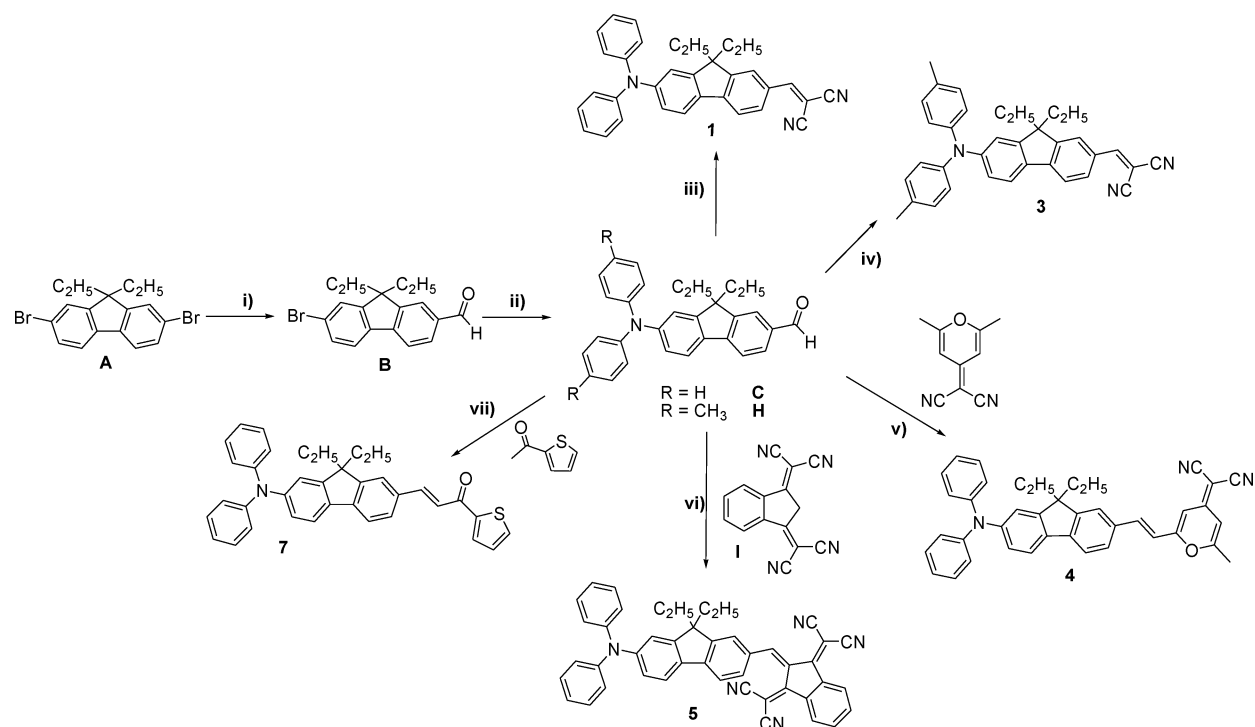
Whereas considerable effort invested in the development of new donor and acceptor groups^{24–26} has led to major progress in the synthesis of stable and efficient chromophores, the relationships between the structure of the π -conjugated spacer and the nonlinear optical properties remain less clearly understood. Our interest in the control of the electronic properties of fluorene-based π -conjugated systems resulted in various synthetic approaches for enhancement of the 2PA cross section based on linear symmetrical and unsymmetrical fluorene chromophores^{27–31} and, recently, two-dimensional branched fluorene-based chromophores.³²

The aromatic character of the fluorene ring can be strongly influenced by the presence of donor or acceptor moieties

Received: November 13, 2012

Published: January 10, 2013

Chart 1

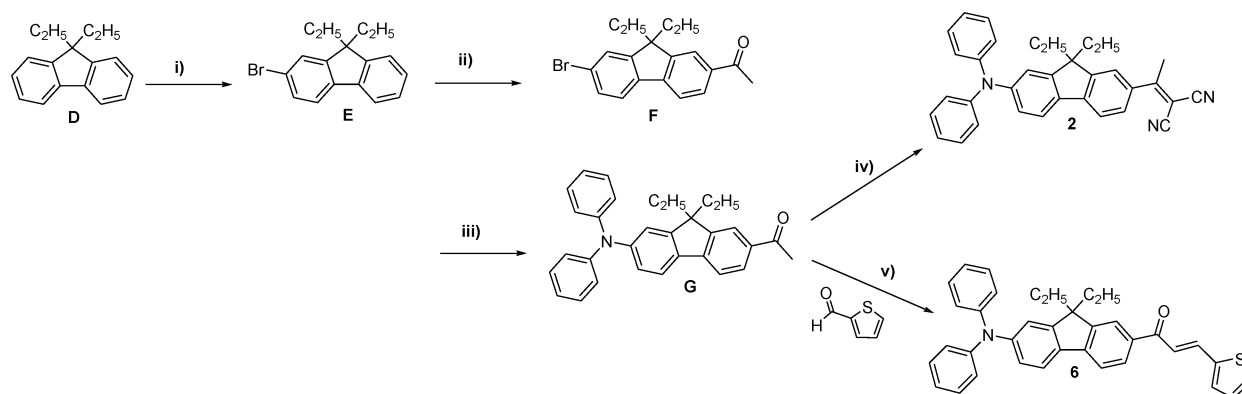
Scheme 1^a.

^aLegend: (i) *n*-BuLi, THF, DMF; (ii) diphenylamine or di-*p*-tolylamine, Pd(OAc)₂, Cs₂CO₃, P(*t*-Bu)₃, toluene; (iii) and (iv) malononitrile, toluene, 70 °C; (v) piperidine, EtOH, reflux; (vi) (CH₃CO)₂O; (vii) KOH, MeOH/H₂O, reflux.

covalently attached at the 2- and 7-positions. Herein, we have employed this approach in the modification of ground-state polarization by altering the strength of the electron-withdrawing terminal group on a fluorene core using four different electron-acceptor groups that are end-capped with a diphenylamine or di-*p*-tolylamine donating group. Electron-withdrawing

groups include 2-pyran-4-ylidene malononitrile, dicyanovinyl, bis(dicyanomethylidene)indane, (thiophen-2-yl)propenone, and dicyanoethylenyl (1–7, Chart 1).

In order to determine the electronic and geometrical properties of compounds 1–7, a comprehensive investigation was conducted by a combination of spectroscopic techniques,

Scheme 2^a.

^aLegend: (i) NBS, propylene carbonate; (ii) AlCl₃, acetyl chloride, 20 h; (iii) Pd(OAc)₂, Cs₂CO₃, P(*t*-Bu)₃, toluene, 22 h; (iv) malononitrile, TiCl₄, pyridine, CHCl₃, (v) KOH, MeOH/H₂O, reflux.

single-crystal X-ray diffraction, and quantum chemical calculations.

RESULTS AND DISCUSSION

Synthesis. The series of new compounds under discussion are shown in Chart 1. All seven push–pull chromophores consist of an amino functionality as the donor and four different electron-acceptor moieties.

The syntheses of the fluorene derivatives are presented in Schemes 1 and 2. The key step in the synthesis of compounds 1–3 and 5 was the Knoevenagel condensation of aldehyde derivatives with the active methylene group of malononitrile. All these dyes were prepared according to a general synthetic methodology involving lithiation of 2,7-dibromo-9,9-diethyl-9H-fluorene with a stoichiometric amount of *n*-BuLi, followed by reaction with dimethylformamide (DMF) and subsequent acidic hydrolysis, providing intermediate B. Arylation of 7-bromo-9,9-diethylfluorene-2-carbaldehyde B was readily performed using Buchwald–Hartwig amination coupling in the presence of a Pd catalyst and a non-nucleophilic base, Cs₂CO₃, to afford intermediate C.³³ Knoevenagel condensation between the resulting aldehyde C with active malononitrile provided compound 1 as a red solid (Scheme 1).

Compound F was obtained in three steps involving C-alkylation of fluorene to give D. Monobromination of D with NBS provided 2-bromo-9,9-diethylfluorene (E), which yielded the acetylated derivative F after a Friedel–Crafts acetylation. The dicyanovinyl derivative 2 was synthesized from the keto derivative F by condensation with malononitrile in the presence of TiCl₄ in pyridine (Scheme 2). After purification, 2 was obtained as orange crystals in 82% yield.

The di-*p*-tolylamine group was used as an electron-donor group in 3 (Scheme 1). The di-*p*-tolylamine group was coupled to 7-bromo-9,9-diethylfluorene-2-carbaldehyde B via a Buchwald–Hartwig arylation, producing fluorenyl aldehyde H. Finally, malononitrile was condensed, via Knoevenagel conditions, with H, affording 3 as a red solid. ¹H NMR showed the presence of a singlet at 2.34 ppm assigned to the methyl groups of the *p*-tolylamine moiety and no aldehydic proton signal.

The versatility of intermediate C was demonstrated in the synthesis of another chromophore comprised of pyranone as an electron-acceptor group. The condensation between C and (2,6-dimethyl-4H-pyran-4-ylidene)malononitrile was carried

out in the presence of piperidine in ethanol, rendering the trans chromophore. The condensation reaction of the (2,6-dimethyl-4H-pyran-4-ylidene)malononitrile with aldehyde C resulted in 4 (Scheme 1), easily separated via column chromatography as a red solid. The two cyano groups of 2-pyran-4-ylidene malononitrile are electron-withdrawing groups, and the electron-deficient pyran ring can act as an auxiliary acceptor.

The indane derivative, 2,2'-(1H-indene-1,3(2H)-diylidene)-dimalononitrile (I), was prepared by reacting 1,3-indanedione and malononitrile in ethanol.³⁴ The conditions used for the final Knoevenagel condensation between intermediate C and I was carried out by reflux in acetic acid for 3 h, providing 5 in high yield as a dark blue solid (Scheme 1).

The thiophen-2-yl-prop-2-en-1-one electron-withdrawing group was introduced by Claisen–Schmidt condensation between thiophene-2-carbaldehyde and compound G, affording chromophore 6 as a yellow solid (Scheme 2). Compound H reacted with 1-(thiophen-2-yl)ethanone, affording chromophore 7 as a yellow solid (Scheme 1). All compounds were characterized by ¹H and ¹³C NMR, mass spectrometry, and elemental analysis.

Linear Photophysical Properties. The dipolar molecules 1–7 possess absorption spectra with two distinct peaks in nonpolar solvents, the main band lying within the range 410–630 nm and the second positioned between 305 and 345 nm (Figures 1–7, curve 1). Excitation anisotropy is correlated with the spectral position of various electronic transitions and can be a very useful tool to estimate the position of 2PA allowed transitions.^{27,35} The locations of these electronic transitions over the spectral range 300–550 nm were revealed from excitation anisotropy. The optical properties of compounds 1–7 are given in Table 1.

In comparing the linear absorbance spectra of this series of compounds, it is noticeable that incorporation of bis-(dicyanovinyl)indane in 5 resulted in the largest red shift relative to compounds 1–4, 6, and 7, indicative of improved charge-transfer characteristics of this donor–acceptor substituted fluorene. To further evaluate the effect of the different electron acceptors on the linear optical properties, 3-(thiophen-2-yl)propanone was used as a benchmark acceptor group, due to this moiety being the weakest acceptor in the series. Absorption at λ_{max} was found to progressively shift to longer wavelength upon replacing this benchmark by dicyano-

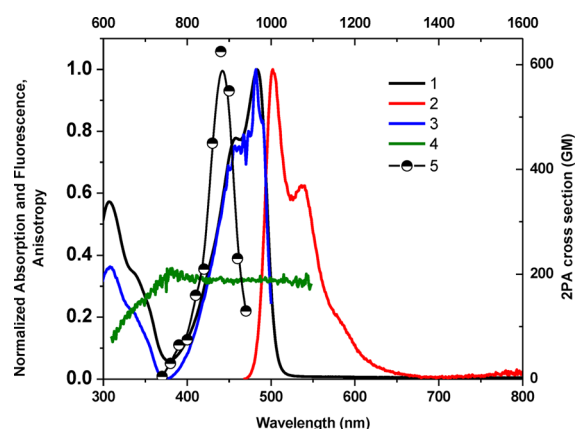


Figure 1. Normalized absorption (1), emission (2), and excitation spectra (3) of **1** in cyclohexane and fluorescence excitation anisotropy (4) in polyTHF. The 2PA spectrum (5) was obtained by the 2PF method in cyclohexane.

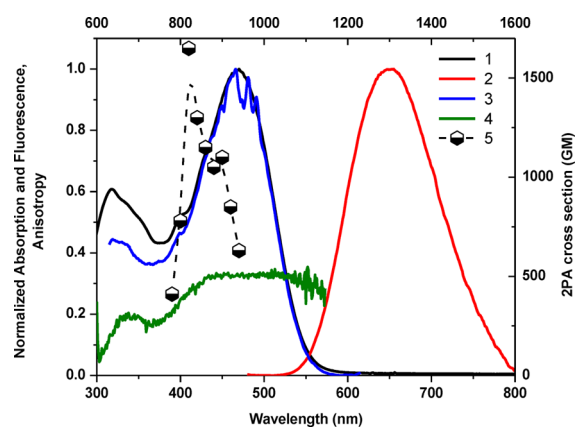


Figure 4. Normalized absorption (1), emission (2), and excitation spectra (3) of **4** in chloroform and fluorescence excitation anisotropy (4) in polyTHF. The 2PA spectrum (5) was obtained by the 2PF method in chloroform.

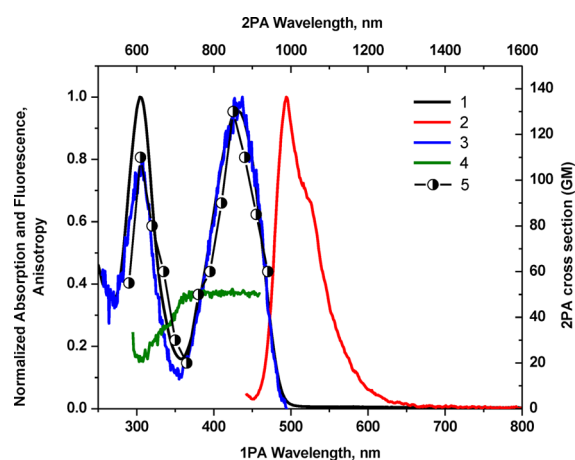


Figure 2. Normalized absorption (1), emission (2), and excitation spectra (3) of **2** in cyclohexane and fluorescence excitation anisotropy (4) in polyTHF. The 2PA spectrum (5) was obtained by the open aperture Z-scan method in cyclohexane.

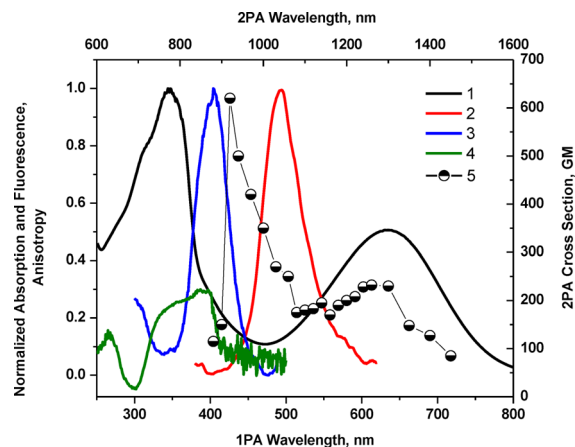


Figure 5. Normalized absorption (1), emission (2), and excitation spectra (3) of **5** in chloroform and fluorescence excitation anisotropy (4) in polyTHF. The 2PA spectrum (5) was obtained by the open aperture Z-scan method in chloroform.

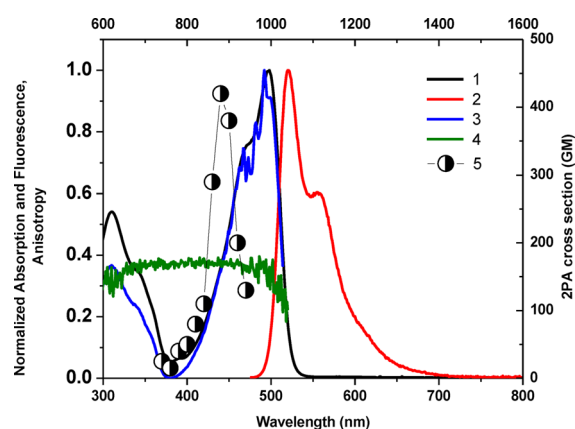


Figure 3. Normalized absorption (1), emission (2), and excitation spectra (3) of **3** in cyclohexane and fluorescence excitation anisotropy (4) in polyTHF. The 2PA spectrum (5) was obtained by the 2PF method in cyclohexane.

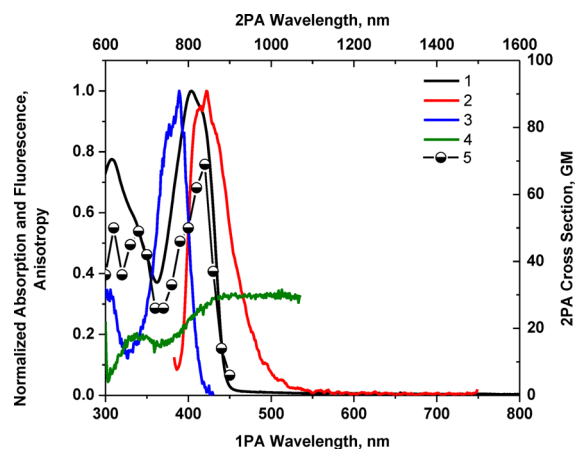


Figure 6. Normalized absorption (1), emission under λ_{exc} 404 nm (2), and excitation spectra (3) of **6** in cyclohexane and fluorescence excitation anisotropy (4) in polyTHF. The 2PA spectrum (5) was obtained by the open aperture Z-scan method in cyclohexane.

methylene and bis(dicyanovinyl)indane (Table 1). A considerable red shift of the main emission bands was observed for chromophores **1**–**7** (Figures 1–7, curve 2). These results

indicate that the fluorescence emission arises from excited state intramolecular charge transfer in these molecules.

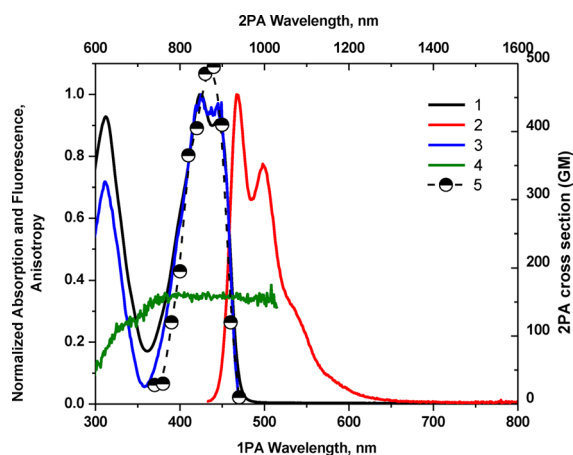


Figure 7. Normalized absorption (1), emission under λ_{exc} 423 nm (2), and excitation spectra (3) of **7** in cyclohexane and fluorescence excitation anisotropy (4) in polyTHF. The 2PA spectrum (5) was obtained by the 2PF method in cyclohexane.

These compounds also displayed pronounced positive solvatochromism (i.e., bathochromic shift with increasing solvent polarity) in their emission spectra, whereas only a slight red shift was observed in the absorption spectra (Figure 8) (representative data are shown for **1** only). This solvatochromic behavior is consistent with the charge-transfer characteristics of donor–acceptor substituted fluorene compounds. A large Stokes shift ($\Delta\lambda_{\text{st}}$) was observed for **4** in CHCl_3 (Figure 4) due to strong solvent–solute dipole–dipole interactions, as a manifestation of the large dipole moment and orientational polarizability in CHCl_3 ($\Delta f \approx 0.152$).

Compounds **1–7** exhibited single-exponential fluorescence decay processes with lifetimes (τ) that were independent of the excitation wavelength over a broad spectral range (280–440 nm).

Quantum yields, Φ , were determined using a fluorescence method,³⁵ exciting at the absorption maximum ($\lambda_{\text{max}}^{\text{Abs}}$) of each molecule. Derivatives **1**, **3**, **4**, and **7** exhibited good Q values in cyclohexane and CHCl_3 (0.31–0.66). Significant deviations from planarity of the electron-acceptor group can explain the largest red shift observed in the absorption spectrum of **5** and may explain the lack of any detectable fluorescence upon excitation at the long-wavelength maximum.

The anisotropy excitation spectra and anisotropy values (r_0) for **1–7** in polyTHF are shown in curve 4 in Figures 1–7. Constant anisotropy values (r_0) for **1–7** in the spectral regions of excitation wavelength, $\lambda_{\text{exc}} \geq 430$ –495 nm (compounds **1–4**, curve 4) and $\lambda_{\text{exc}} \geq 405$ –425 nm (compounds **6** and **7**),

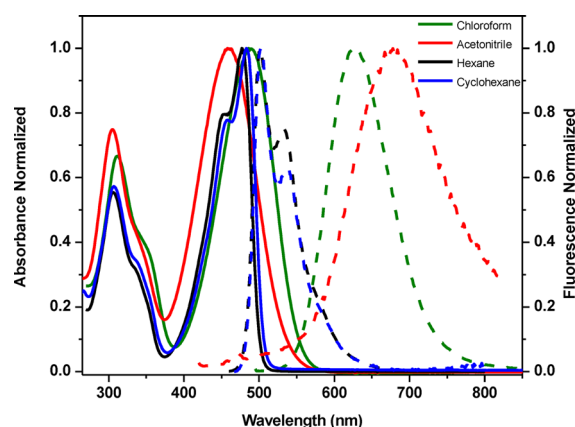


Figure 8. Normalized absorption (solid lines) and emission spectra (dashed lines) for **1** in different solvents.

correspond to the main absorption band ($S_0 \rightarrow S_1$ transition), while the change in anisotropy for compound **5** under excitation in the short-wavelength absorption band (λ_{exc} 345 nm) exhibited a complicated electronic structure of the main long-wavelength absorption band.

Nonlinear Photophysical Properties. The 2PA spectra for compounds **1–7** are shown as curve 5 in Figures 1–7. 2PA spectra for compounds **1**, **3**, **4**, and **7** were acquired using the 2PF technique over a broad spectral region, 740–940 nm, since they possessed high fluorescence quantum yields. 2PA spectra were measured for compounds **2**, **5**, and **6** by open aperture Z-scan methods due to their low fluorescence quantum yields. The maxima of 2PA cross section (δ) values for **1–7** were at ca. 880 nm, close to a linear absorption maximum at ca. 440 nm and attributed to the $S_0 \rightarrow S_1$ transition (identified by both linear absorption and anisotropy spectra), a formally forbidden transition for 2PA. The peak position of the 2PA spectra of **2**, **6**, and **7** correlated quite well with the position of the transition to the first excited state for this system, as indicated by the location of the long-wavelength band in the linear absorption spectrum (440 nm). Because these molecules do not possess a center of symmetry, it is not surprising that each of the low-lying transitions ($S_0 \rightarrow S_1$ and $S_0 \rightarrow S_2$) are observed by two-photon absorption.

As expected, from the linear absorption analysis, the value of λ_{max} did vary significantly with the strength of the electron-withdrawing moiety. There was no strong deviation of the λ_{max} values in 2PA spectra with changes in the electron-withdrawing group. Compound **4** contained a pyran group and exhibited a nearly 3-fold enhancement of δ (1650 GM at 840 nm) relative

Table 1. Main Photophysical Parameters of Compounds **1–7**: Absorption ($\lambda_{\text{max}}^{\text{Abs}}$) and Fluorescence Maxima ($\lambda_{\text{max}}^{\text{Fl}}$), Stokes Shift ($\Delta\lambda_{\text{st}}$), Maximum Extinction Coefficient (ϵ^{max}), Fluorescence Quantum Yield (Φ), Anisotropy (r_0), and Fluorescence Lifetime (τ)

compd	$\lambda_{\text{max}}^{\text{Abs}}$	$\lambda_{\text{max}}^{\text{Fl}}$	$\Delta\lambda_{\text{st}}$	$\epsilon^{\text{max}}, 10^{-3} \text{ M}^{-1} \text{ cm}^{-1}$	Φ	$r_0(\text{p-THF})$	τ (ns)
1 ^a	483 ± 1	502 ± 1	19	50	0.31 ± 0.05	0.32	1.00 ± 0.01
2 ^a	430 ± 1	495 ± 1	65	29	0.02 ± 0.05	0.36	0.13 ± 0.08
3 ^a	498 ± 1	520 ± 1	22	54	0.66 ± 0.05	0.37	1.95 ± 0.05
4 ^b	470 ± 1	648 ± 1	178	79	0.64 ± 0.05	0.32	2.8 ± 0.01
5 ^b	345, 634 ± 1	500 ± 1 ^c		24	0.001 ± 0.05	0.30	
6 ^a	404 ± 1	420 ± 1	16	40	0.01 ± 0.05	0.22	0.21 ± 0.09
7 ^a	423 ± 1	468 ± 1	45	27	0.49 ± 0.05	0.35	1.37 ± 0.02

^aAbsorption and emission spectra measured in cyclohexane. ^bAbsorption and emission spectra measured in chloroform. ^cExcited at 345 nm.

to the rest of the series (see curves 5 in Figures 1–7). This is particularly intriguing, considering that in this series the bis(dicyanomethylidene)indane accepting group was assumed to be the strongest electron-withdrawing group in comparison to the other substituents studied.

Thus, the study of the dipolar fluorene derivatives illustrates that there appears to be an optimum degree of ground-state polarization that maximizes δ . Furthermore, it does not necessarily correspond to the molecule which possesses the strongest ground-state dipole moment (as revealed by quantum calculations (Table S1, Supporting Information), as **4** possesses the largest dipole moment in the series). As a result, fluorenyl **4**, with its pyranone terminal group, has optimal charge transfer character that maximizes its state and transition dipole moments, the main factors that influence the strength of 2PA.

Single-Crystal X-ray Structural Analysis. Crystals suitable for single crystal X-ray analysis were obtained for compounds **1**, **2**, and **6** by the slow diffusion of hexane into a concentrated dichloromethane solution. Solid-state structural analysis for the fluorene-containing compounds has generally been rarely reported, due, in part, to difficulties in growing single crystals. Single-crystal X-ray structural analysis was completed for compounds **1**, **2**, and **6** (Table 2). Single crystals could not be obtained for the other compounds in the series.

Table 2. Summary of the Crystal Data and Structure Refinement Parameters for 1, 2, and 6

	1	2	6
formula	C ₃₃ H ₂₇ N ₃	C ₃₄ H ₂₉ N ₃	C ₃₆ H ₃₁ NOS
formula wt	465.58	479.60	525.69
cryst syst	triclinic	triclinic	triclinic
space group	P $\bar{1}$	P $\bar{1}$	P $\bar{1}$
a/Å	8.3392(13)	8.7255(12)	9.3797(6)
b/Å	10.0974(16)	10.8750(15)	10.4703(6)
c/Å	15.684(3)	15.855(2)	15.9304(10)
α /deg	98.756(2)	98.469(2)	79.5150(10)
β /deg	101.508(2)	101.687(2)	78.4040(10)
γ /deg	97.415(2)	110.096(2)	67.3940(10)
V/Å ³	1261.5(4)	1344.6(3)	1405.30(15)
Z	2	2	2
D _c /Mg m ⁻³	1.226	1.185	1.242
μ (Mo K α)/mm ⁻¹	0.072	0.070	0.145
F(000)	492	508	556
no. of collected/unique rflns (R(int))	16761/6046 (0.0645)	14513/4732 (0.0434)	15012/4944 (0.0310)
no. of rflns with I > 2 σ (I)	3370	4732	4944
goodness of fit on F ²	1.001	1.012	1.043
R, R _w (I > 2 σ (I))	0.0585, 0.1293	0.0399, 0.0876	0.0407, 0.0988

The fluorene substructure is essentially planar for all three compounds. Phenyl rings from the diphenylamino donor group are twisted with respect to the fluorene bridge; angles range from 60.8(1) to 67.8(1)° (Table 3). Similar values were observed for analogous unsymmetrical fluorene-based derivatives.³³

The nitrogen in the diphenylamino group exhibited a trigonal-planar environment in **1**, showing a slight deviation to a pyramidal configuration in analogues **2** and **6**, with C–N–C angles being in the range of 116.7(2)–121.7(2)°. The largest deviation from the plane formed by C(11), C(18), and C(19)

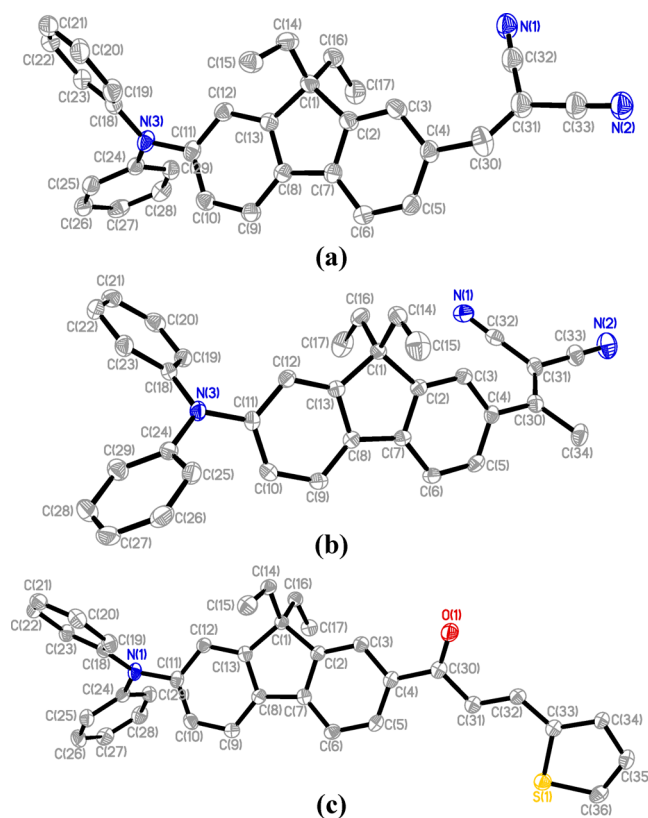


Figure 9. ORTEP drawings for **1** (a), **2** (b), and **6** (c) with the numbering scheme. Thermal ellipsoids are shown at the 50% probability level. Only the major part of the disordered dicyanovinyl fragment in **1** is shown. Hydrogen atoms are omitted for clarity.

carbons was 0.119(2) Å, suggesting sp² hybridization of the N atom and, consequently, donation of its pair of nonbonding electrons into the π conjugation chromophore system (Table 3). The molecular geometry of **1** revealed both syn (major disordered part) and trans (minor part) conformations of the dicyanovinyl group (see the Experimental Section), with the values for the torsion angle C(3)–C(4)–C(30)–C(31) being 30.1(4) and 161.1(5)°, respectively. Compound **2** clearly exhibited a syn conformation of the dicyanovinyl group, with the torsion angle C(3)–C(4)–C(30)–C(31) equal to 42.5(2)°. Compound **6** revealed the largest deviation from planarity for the acceptor group, manifested by the torsion angle C(5)–C(4)–C(30)–C(31) of 18.6(3)°, due to H···H repulsion interactions of H atoms attached to C(5) and C(31).

The crystal packing in **1**, **2**, and **6** was determined by antiparallel dipole–dipole interactions between the molecules related by inversion centers. The bulky diphenylamino group and essentially eclipsed ethyl substituents on the fluorene moiety prevent any close π – π intermolecular interactions (Figure S1, Supporting Information).

Quantum Chemical Calculations. Ground-state optimized geometries show only slight differences in comparison to available crystallographic data. The nitrogen atom in the diarylamine group became essentially coplanar with the bonded carbon atoms, suggesting improved electron donation to the fluorenyl π system. The torsion angle C(3)–C(4)–C(30)–C(31), describing syn isomerization in **1** and **2**, arrived at values of 0.2 and 35.9°, respectively. The fluorene core and the acceptor group were positioned essentially in the same plane for the optimized geometries of **4** and **7**. The bis(dicyanovinyl)-

Table 3. Selected Structural Parameters (\AA , deg) for Experimental (x) and Calculated (c) Molecules

molecule	P_A-P_B	P_A-P_C	N^a	C(11)–N(3)–C(18)	C(18)–N(3)–C(24)	C(24)–N(2)–C(11)
1c	60.55	82.94	0.032	119.94	121.43	118.48
1x	60.60(5)	82.95(5)	0.032(2)	119.9(2)	121.4(2)	118.5(2)
2c	69.55	67.86	0.003	120.33	119.04	120.63
2x	63.09(4)	72.87(4)	0.118(2)	119.7(1)	119.4(1)	118.8(1)
3c	68.98	66.93	0.006	120.67	118.34	120.99
4c	70.18	68.84	0.003	120.24	119.29	120.47
5c	69.07	67.76	0.003	120.57	118.60	120.83
6c	70.54	68.89	0.003	120.11	119.48	120.41
6x	67.75(5)	81.85(5)	0.119(2)	119.6(2)	121.7(2)	116.7(2)
7c	70.41	68.91	0.003	120.14	119.47	120.39

^aDeviation of the central nitrogen atom from its bonded neighboring carbon atoms.

indane acceptor in **5** had a distorted geometry due to steric repulsions between dicyanovinyl groups and the fluorene core, with an angle at the bridging C sp^2 atom equal to 132.1° (Figure 10) and an interplanar angle between the fluorene core and bis(dicyanovinyl)indane group of 38.8° .

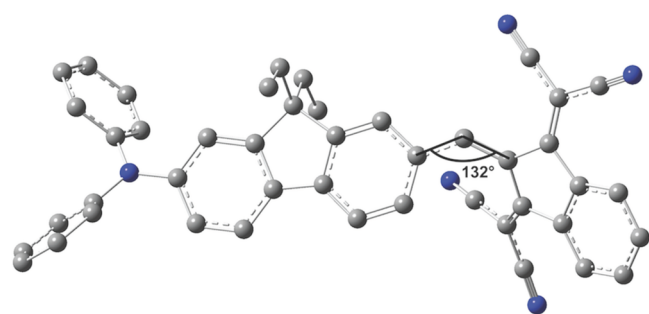


Figure 10. DFT optimized geometry of **5**.

The electron acceptor group in **6** deviated from the best plane with a C(5)–C(4)–C(30)–C(31) torsion angle value equal to 8.0° , due to H··H repulsion mentioned in the crystallographic description. The comparison of ground state dipole moment values is an indicator of the donor–acceptor strengths of the studied systems. Both functionals (B3LYP and M06) showed similar tendencies in dipole moments (Table S1, Supporting Information). With addition of the methyl group to the terminal phenyl rings, the dipole moment increased

(compare compounds **1** and **3**). This result can be explained by the hyperconjugation effect. The methyldiene malononitrile group (**1**) showed slightly stronger acceptor properties in comparison to ethylidene malononitrile (**2**). Fluorenyl **4**, with a pyronone group as an electron acceptor, possessed the largest dipole moment in the series, suggesting enhanced linear and nonlinear absorption properties. The nonplanarity observed in **6** led to a decrease in conjugation and, as a result, a slightly decreased dipole moment in comparison to **7**.

Singlet Excited States. Two main bands in the absorption spectra of **1–7** are well reproduced by time-dependent (TD) DFT calculations (Table 4).

As was recently validated for fluorene-based push–pull chromophores, 2PA in the lowest energy transition correlates with the values of the transition dipole moment and permanent dipole moment differences between the ground and first excited states ($S_0 \rightarrow S_1$).^{36,37} Therefore, only the lowest energy electronic excitation is considered below. The calculated absorption maxima were in good agreement with those experimentally observed, providing credence to the computational method. As revealed by TD DFT calculations, the ground to first excited state transition described the lowest lying energy excitation. Red shifts observed in the absorption spectra are well reproduced by the calculations, suggesting increased intramolecular charge transfer (CT) character along the series. However, bis(dicyanovinyl)indane in diphenylaminofluorene **5** resulted in the largest red shift relative to the rest of the compounds but did not lead to improved CT

Table 4. Calculated Ground Energy and Dipole (E_g (eV) and μ_g (D)) and Excited State (λ_c (nm), f , μ_t (D)) Properties at the M06/6-311++G** Level

	λ_c	f	transition	μ_t	μ_g	E_g
1	346	0.3696	$S_0 \rightarrow S_2$	4.2122	9.9395	–39110.0516632424
	488	0.7821	$S_0 \rightarrow S_1$	12.5691		
2	334	0.3583	$S_0 \rightarrow S_3$	3.9441	8.2282	–40179.3249837085
	469	0.6005	$S_0 \rightarrow S_1$	9.2694		
3	362	0.4713	$S_0 \rightarrow S_2$	5.6102	10.8632	–41248.562096415
	531	0.9627	$S_0 \rightarrow S_1$	16.8228		
4	391	0.7373	$S_0 \rightarrow S_2$	9.4835	13.5913	–48546.3220781635
	501	1.1375	$S_0 \rightarrow S_1$	18.7683		
5	360	0.3693	$S_0 \rightarrow S_7$	4.3732	7.4602	–54630.8843510249
	652	0.5087	$S_0 \rightarrow S_1$	10.9133		
6	352	0.5553	$S_0 \rightarrow S_3$	6.4272	2.3721	–52188.2893297265
	448	0.6647	$S_0 \rightarrow S_1$	9.8138		
7	341	0.6301	$S_0 \rightarrow S_4$	7.0807	4.1917	–52188.3070881576
	451	0.8977	$S_0 \rightarrow S_1$	13.3268		

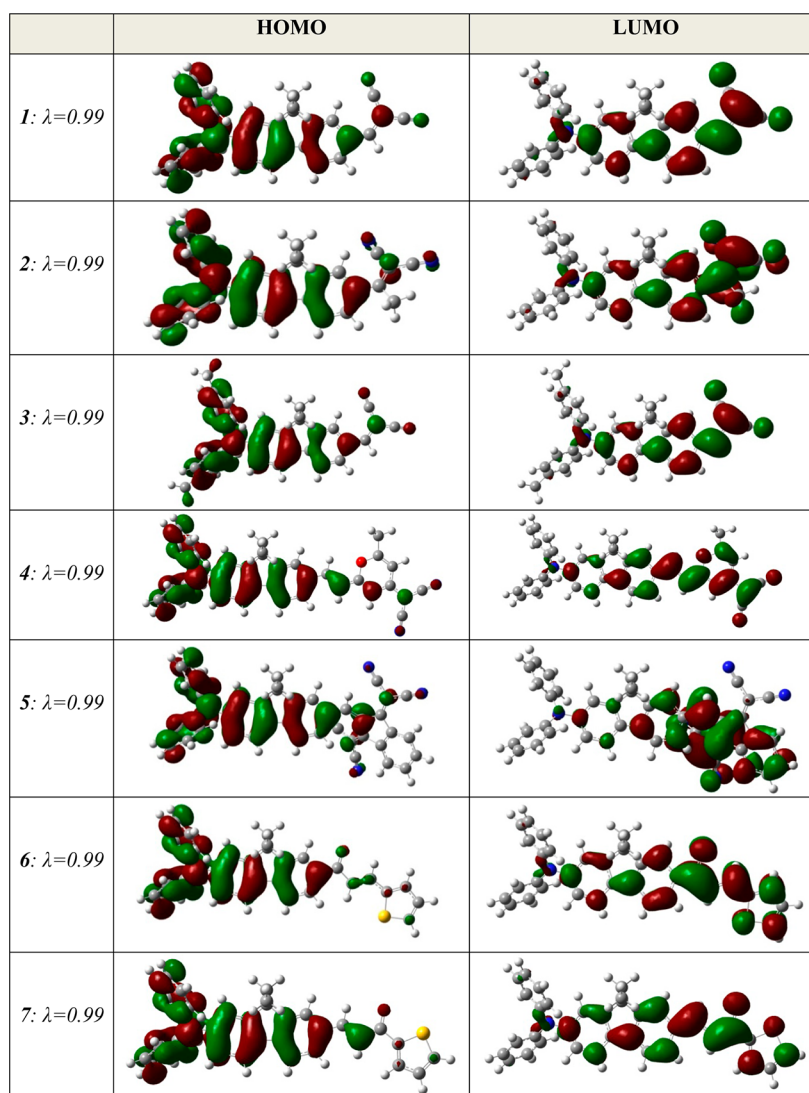


Figure 11. $S_0 \rightarrow S_1$ natural transition orbitals. λ is the fraction of the NTO pair contribution into the given electronic excitation.

characteristics, as revealed by ground and transition dipole moments, as well as by natural transition orbital (NTO) analysis. Improvement of CT correlates well with the increase of the both ground and transition dipole moment values. Enhanced hyperconjugation results in slightly improved CT for **3** over **1**. Fluorenyl thiophene **6**, having the weakest acceptor group (thiophen-2-yl prop-2-en-1-one), revealed the shortest λ_{\max} and smallest ground state dipole. NTOs for the $S_0 \rightarrow S_1$ transition are shown in Figure 11.

We note several common aspects for the chromophores with regard to transition character: (i) as expected, the HOMO wave function is more developed on the donor, whereas the LUMO wave function is more developed on the acceptor group; (ii) electron density redistribution clearly suggests $\pi \rightarrow \pi^*$ transition character, except the small fraction of $\sigma \rightarrow \pi^*$ coming from donor methyl groups (when present); (iii) ethyl groups located on fluorene are not involved in CT whatsoever; (iv) finally, because of the existence of an overlap of the HOMO and LUMO wave functions, transition cannot be attributed to pure CT character. The largest transition dipole moment observed for **4** is mirrored by the LUMO wave function, which is even less pronounced on the diphenylamino group in this compound in comparison to the other molecules.

For **5**, the LUMO wave function is located mainly on the aromatic portion, not on the dicyanovinyl moiety of the acceptor.

CONCLUSIONS

In summary, modification of diphenylaminofluorene by the introduction of electron-withdrawing groups resulted in a series of robust two-photon absorbing fluorene-based chromophores. It was found that the absorption and emission spectra show significant bathochromic shifts according to the strength of the electron-withdrawing moieties. Compound **4**, with its pyranone terminal group, showed the optimal charge transfer character in this series of compounds, which maximizes its state and transition dipole moments (it had the largest transition dipole moment), and exhibited the largest 2PA cross-section values. Data from linear and nonlinear photophysical studies, crystallographic studies, and quantum mechanical calculations were relatively consistent and provided insight into the observed behavior of the molecules. It was shown that there is an optimum degree of dipolar molecular character, with the strongest electron-withdrawing group not necessarily providing the largest 2PA. Results from this study provide the rationale to

design 2PA materials for applications such as probes for two-photon fluorescence bioimaging applications.

EXPERIMENTAL SECTION

Materials and Methods. 2,7-Dibromo-9,9-diethylfluorene (A), 9,9-diethylfluorene (D), 2-bromo-9,9-diethyl-9H-fluorene (E), and 1,3-bis(dicyanomethylene)indane (I) were prepared as described previously.^{30,38,34} Reactions were carried out under a N₂ or Ar atmosphere. THF was freshly distilled from Na and benzophenone ketyl. AlCl₃ was purified by sublimation before use. All other reagents and solvents were used as received from commercial suppliers. ¹H and ¹³C NMR spectra were recorded on an NMR spectrometer at 500 and 125 MHz, respectively, with reference to TMS at 0.00 ppm.

Synthesis of 7-Bromo-9,9-diethylfluorene-2-carbaldehyde (B). Under a nitrogen atmosphere and at -78 °C, *n*-BuLi (3.28 mL, 1.6 M in hexanes) was added dropwise over 20 min to a dry THF solution (15 mL) containing 2,7-dibromo-9,9-diethylfluorene (2 g, 5.26 mmol). After 1 h of stirring, 0.58 mL of DMF was added slowly to the reaction solution. After another 2 h of stirring, the solution was brought back to room temperature and the reaction was quenched with 2 N HCl. The solution was extracted with toluene and subjected to flash column chromatography (silica gel, hexanes/ethyl acetate 4/1). A white solid was obtained. Yield: 89% (1.52 g). Mp: 124–125 °C (lit.³⁸ mp 126–128 °C). ¹H NMR (500 MHz, CDCl₃): δ 9.77 (s, 1H), 7.57 (s, 2H), 7.53 (d, *J* = 7 Hz, 1H), 7.36 (d, *J* = 8.5 Hz, 1H), 7.23–7.21 (m, 2H), 1.83–1.72 (m, 4H), 0.3 (t, *J* = 10 Hz, 6H). ¹³C NMR (125 MHz, CDCl₃): δ 192.3, 153.4, 150.3, 146.7, 138.9, 135.6, 130.6, 130.3, 126.7, 126.4, 123.2, 123.1, 120.0, 56.6, 32.5, 8.4 ppm.

Synthesis of 7-(Diphenylamino)-9,9-diethylfluorene-2-carbaldehyde (C). Under a nitrogen atmosphere, a mixture of 7-bromo-9,9-diethylfluorene-2-carbaldehyde (3 g, 9.11 mmol), diphenylamine (2.31 g, 13.66 mmol), Pd(OAc)₂ (0.05 g, 0.22 mmol), P(tBu)₃ (0.1 g, 0.49 mmol), and Cs₂CO₃ (4.45 g, 13.65 mmol) in toluene (20 mL) was stirred and heated at 120 °C for 24 h. After it was cooled to room temperature, the reaction mixture was passed through a short plug (silica gel) and the filtrate was concentrated to give a brown oil. Purification was carried out by flash column chromatography (silica gel, first hexanes, then hexanes/ethyl acetate 4/1). A yellow solid was obtained. Yield: 88% (3.31 g). Mp: 156–157 °C. ¹H NMR (500 MHz, CDCl₃): δ 9.69 (s, 1H), 7.50 (dd, *J* = 7.5 Hz, 2H), 7.40 (dd, *J* = 8 Hz, 1H), 7.30 (dd, *J* = 8.5 Hz, 1H), 6.97–6.93 (m, 4H), 6.81 (dd, *J* = 6.5 Hz, 4H), 6.77 (d, *J* = 2 Hz, 1H), 6.74–6.71 (m, 4H), 1.72–1.65 (m, 2H), 1.61–1.53 (m, 2H), 0.02 (t, *J* = 14.5, 6H). ¹³C NMR (125 MHz, CDCl₃): δ 192.2, 152.8, 150.5, 148.9, 147.9, 147.6, 134.5, 134.3, 138.9, 129.3, 124.4, 123.1, 122.9, 121.69, 119.1, 118.1, 56.1, 32.4, 8.5 ppm. HRMS (ESI-TOF): *m/z* [M + H]⁺ calcd for C₃₀H₂₈NO 418.2165, found 418.2176.

Synthesis of 2-((2-(Diphenylamino)-9,9-diethylfluorene-7-yl)methylene)malononitrile (1). 7-(Diphenylamino)-9,9-diethylfluorene-2-carbaldehyde (0.4 g, 0.96 mmol), malononitrile (0.12 g, 1.92 mmol), and basic aluminum oxide (0.45 g) were stirred in toluene (5 mL) for 24 h at 70 °C. After it was cooled to room temperature, the reaction solution was filtered. The filtrate was subjected to column chromatography (silica gel, hexanes/ethyl acetate 9/1). A red solid was obtained. Yield: 91% (0.40 g). Mp: 189–190 °C. ¹H NMR (500 MHz, CDCl₃): δ 7.89 (d, *J* = 2 Hz, 1H), 7.83 (dd, *J* = 8 Hz, 1H), 7.76 (s, 1H), 7.69 (d, *J* = 8 Hz, 1H), 7.61 (d, *J* = 8 Hz, 1H), 7.31–7.25 (m, 4H), 7.15 (bd, *J* = 8 Hz, 4H), 7.09 (m, 4H), 2.02–1.99 (m, 2H), 1.98–1.85 (m, 2H), 0.38 (t, *J* = 15 Hz, 6H). ¹³C NMR (125 MHz, CDCl₃): δ 159.9, 159.8, 153.3, 151.0, 149.7, 148.6, 147.4, 133.5, 131.6, 129.5, 124.9, 124.7, 124.5, 124.4, 123.6, 123.5, 122.4, 122.3, 122.11, 122.0, 119.6, 119.5, 117.4, 114.6, 113.6, 79.1, 56.3, 32.3, 8.5 ppm. HRMS (ESI-TOF): *m/z* [M + H]⁺ calcd for C₃₃H₂₈N₃ 466.2278, found 466.2274.

Synthesis of 1-(2-Bromo-9,9-diethyl-9H-fluorene-7-yl)ethanone (F). To a solution of AlCl₃ (4.09 g, 30.71 mmol) in 115 mL of CH₂Cl₂ was added acetyl chloride (2.08 mL) under a nitrogen atmosphere at 0 °C. Then 18 mL of 2-bromo-9,9-diethyl-9H-fluorene (8.1 g, 26.89 mmol) dissolved in 17 mL of CH₂Cl₂ was added at the same temperature. After it was stirred at room temperature for 20 h,

the solution was poured into cold water. The separated organic phase was dried over Na₂SO₄. The product was purified by column chromatography using a hexane/ethyl acetate mixture (4/1). A white solid was isolated. Yield: 78% (7.2 g). Mp: 120–121 °C. ¹H NMR (500 MHz, CDCl₃): δ 7.97 (t, *J* = 7.5 Hz, 2H), 7.74 (d, *J* = 8 Hz, 1H), 7.63 (d, *J* = 8 Hz, 1H), 7.51–7.49 (m, 2H), 2.66 (s, 3H), 2.11–1.99 (m, 4H), 0.31 (t, *J* = 15 Hz, 6H). ¹³C NMR (125 MHz, CDCl₃): δ 198.0, 153.3, 149.8, 145.3, 139.1, 136.2, 130.5, 128.4, 126.6, 122.6, 122.4, 121.9, 119.5, 56.7, 32.5, 27.0, 8.4 ppm. HRMS (ESI-TOF): *m/z* [M + Na]⁺ calcd for C₁₉H₁₉BrONa 365.0511, found 365.0514.

Synthesis of 1-(2-(Diphenylamino)-9,9-diethyl-9H-fluorene-7-yl)ethanone (G). Under a nitrogen atmosphere, a mixture of 1-(2-bromo-9,9-diethyl-9H-fluorene-7-yl)ethanonecarbaldehyde (6 g, 17.47 mmol), diphenylamine (4.43 g, 26.20 mmol), Pd(OAc)₂ (0.13 g, 0.59 mmol), P(tBu)₃ (0.21 g, 1.06 mmol), and Cs₂CO₃ (8.33 g, 25.56 mmol) in toluene (55 mL) was stirred and heated at 120 °C for 36 h. After it was cooled to room temperature, the reaction mixture was passed through a short plug (silica gel) and the filtrate was concentrated, giving a yellow brownish oil. Purification was carried out by column chromatography (silica gel, hexanes/CH₂Cl₂ 3/2). A yellow solid was obtained. Yield: 78% (5.88 g). Mp: 142–143 °C. ¹H NMR (500 MHz, CDCl₃): δ 7.94 (dd, *J* = 7.5 Hz, 1H), 7.90 (s, 1H), 7.65 (d, *J* = 8 Hz, 1H), 7.61 (d, *J* = 8.5 Hz, 1H), 7.28 (t, *J* = 5.5 Hz, 4H), 7.14 (d, *J* = 5.5 Hz, 4H), 7.10 (d, *J* = 2 Hz, 1H), 7.05 (t, *J* = 7.5 Hz, 3H), 2.64 (s, 3H), 2.03 (m, 2H), 1.91 (m, 2H), 0.34 (t, *J* = 14.5 Hz, 6H). ¹³C NMR (125 MHz, CDCl₃): δ 198.1, 152.6, 150.0, 148.5, 147.7, 146.4, 135.0, 134.7, 129.5, 129.0, 124.5, 124.0, 122.9, 122.3, 121.3, 118.7, 56.2, 32.5, 26.8, 8.5 ppm. HRMS (ESI-TOF): *m/z* [M + H]⁺ calcd for C₃₁H₃₀NO 432.2322, found 432.2323.

Synthesis of 2-(1-(2-(Diphenylamino)-9,9-diethyl-9H-fluorene-7-yl)ethylidene)malononitrile (2). In a reaction flask, 1-(2-(diphenylamino)-9,9-diethyl-9H-fluorene-7-yl)ethanone (0.8 g, 1.85 mmol) and malononitrile (0.26 g, 4.06 mmol) were added under a nitrogen atmosphere, followed by anhydrous chloroform (36 mL) to give a clear yellow solution. It was then added to pyridine (600 mg, 7.58 mmol) and an excess amount of titanium tetrachloride (5.5 mL, 47.65 mmol) with continuous stirring. The reaction mixture immediately turned deep brown. The solution was stirred for 30 min and subsequently quenched with water (100 mL). The liquid was concentrated under vacuum and purified using column chromatography (silica gel) first with CH₂Cl₂ and then with a hexane/CH₂Cl₂ (1/4) solvent mixture as eluent, providing orange crystals. Yield: 73% (0.65 g). Mp: 200–201 °C. ¹H NMR (500 MHz, CDCl₃): δ 7.68 (d, *J* = 8 Hz, 1H), 7.59 (d, *J* = 5.5 Hz, 2H), 7.54 (dd, *J* = 8.5 Hz, 1H), 7.29 (t, *J* = 5.5 Hz, 4H), 7.14 (d, *J* = 5.5 Hz, 4H), 7.08–7.03 (m, 4H), 2.69 (s, 3H), 1.99–1.89 (m, 6H), 0.37 (t, *J* = 15 Hz). ¹³C NMR (125 MHz, CDCl₃): δ 175.1, 152.4, 150.4, 148.9, 147.6, 146.2, 134.1, 133.0, 129.8, 129.6, 129.1, 128.8, 127.1, 126.8, 124.8, 124.1, 123.9, 123.5, 123.1, 122.9, 122.5, 122.2, 121.9, 121.4, 119.3, 118.4, 117.7, 113.6, 113.4, 56.5, 32.4, 24.1, 8.5 ppm. HRMS (ESI-TOF): *m/z* [M + Na]⁺ calcd for C₃₄H₂₉N₃Na 502.2254, found 502.2256.

Synthesis of 7-(Di-*p*-tolylamino)-9,9-diethyl-9H-fluorene-2-carbaldehyde (H). Under a nitrogen atmosphere, a mixture of 7-bromo-9,9-diethylfluorene-2-carbaldehyde (2 g, 6.07 mmol), di-*p*-tolylamine (1.77 g, 9.0 mmol), Pd(OAc)₂ (0.03 g, 0.13 mmol), P(tBu)₃ (0.064 g, 0.32 mmol), and Cs₂CO₃ (2.96 g, 9.1 mmol) in toluene (14 mL) was stirred and heated at 120 °C for 36 h. After cooling to room temperature, the reaction mixture was passed through short plug (silica gel) and the filtrate was concentrated to give a yellow–brown oil. Purification was carried out by flash column chromatography (silica gel, hexanes/CH₂Cl₂ 3:2). A fluorescent yellow solid was obtained. Yield: 70% (1.9 g). Mp: 156–157 °C. ¹H NMR (500 MHz, CDCl₃): δ 10.01 (s, 1H), 7.81 (d, *J* = 8 Hz, 2H), 7.70 (d, *J* = 8 Hz, 1H), 7.57 (d, *J* = 8 Hz, 1H), 7.09–6.96 (m, 10H), 2.33 (s, 6H), 2.02–1.98 (m, 2H), 1.90–1.86 (m, 2H), 0.35 (t, *J* = 15 Hz, 6H) ppm. ¹³C NMR (125 MHz, CDCl₃): δ 192.2, 152.7, 150.3, 149.3, 148.1, 145.1, 134.2, 133.4, 132.8, 130.9, 130.2, 129.9, 124.7, 122.8, 121.6, 121.5, 118.8, 116.8, 56.1, 32.5, 32.4, 20.8, 20.8, 8.4 ppm. HRMS (ESI-TOF): *m/z* [M + H]⁺ calcd for C₃₂H₃₂NO 446.2478, found 446.2479.

Synthesis of 2-((2-(Di-*p*-tolylamino)-9,9-diethylfluoren-7-yl)-methylene)malononitrile (3). 7-(Di-*p*-tolylamino)-9,9-diethyl-9*H*-fluorene-2-carbaldehyde (1.5 g, 3.36 mmol), malononitrile (0.44 g, 6.72 mmol), and basic aluminum oxide (1.58 g) were stirred in toluene (18 mL) for 16 h at 70 °C. After it was cooled to room temperature, the reaction solution was filtered. The filtrate was subjected to column chromatography (silica gel, toluene). A red solid was obtained. Yield: 86% (1.43 g). Mp: 211–212 °C. ¹H NMR (500 MHz, CDCl₃): δ 7.88 (d, *J* = 2 Hz, 1H), 7.82 (dd, *J* = 8.5 Hz, 1H), 7.76 (s, 1H), 7.66 (d, *J* = 8 Hz, 1H), 7.56 (d, *J* = 8.5 Hz, 1H), 7.10 (d, *J* = 8 Hz, 4H), 7.04–7.00 (m, 4H), 6.98 (dd, *J* = 8.5 Hz, 1H), 2.34 (s, 6H), 1.99–1.95 (m, 2H), 1.89–1.85 (m, 2H), 0.37 (t, *J* = 15 Hz, 6H) ppm. ¹³C NMR (125 MHz, CDCl₃): δ 159.8, 153.3, 150.8, 150.1, 148.9, 144.8, 133.3, 132.5, 131.7, 130.1, 128.4, 125.2, 124.3, 122.0, 121.8, 119.4, 116.0, 114.7, 113.7, 78.6, 56.2, 32.3, 20.9, 8.5 ppm. HRMS (ESI-TOF): *m/z* [M + H]⁺ calcd for C₃₅H₃₂N₃ 494.2591, found 494.2582.

Synthesis of (E)-2-(3-(2-(7-(Diphenylamino)-9,9-diethyl-9*H*-fluoren-2-yl)vinyl)-5-methyl-4-oxocyclohexa-2,5-dienylidene)malononitrile (4). A mixture of aldehyde C (0.56 g, 1.35 mmol) and 2,6-dimethyl-4-dicyanomethylene-4*H*-pyran (0.25 g, 1.35 mmol) was dissolved in EtOH (35 mL). After piperidine (0.5 mL) was added slowly through a syringe with stirring, the reaction mixture was refluxed for 72 h. A reddish precipitate was obtained after cooling the reaction mixture to room temperature. Compound 4 was obtained after purifying the product through a silica gel column using hexanes/ethyl acetate (4/1) as eluent. A red solid was obtained. Yield: 35% (0.28 g). Mp: 299–300 °C. ¹H NMR (500 MHz, CDCl₃): δ 7.64 (d, *J* = 8 Hz, 1H), 7.58 (d, *J* = 8 Hz, 1H), 7.54 (s, 1H), 7.51 (d, *J* = 8 Hz, 1H), 7.46 (s, 1H), 7.28–7.25 (m, 5H), 7.14 (d, *J* = 8.5 Hz, 4H), 7.09 (d, *J* = 2 Hz, 1H), 7.05–7.02 (m, 3H), 6.76 (d, *J* = 16 Hz, 1H), 6.70 (d, *J* = 1.5 Hz, 1H), 6.55 (s, 1H), 2.42 (s, 3H), 2.05–1.88 (m, 4H), 0.38 (t, *J* = 14.5 Hz, 6H). ¹³C NMR (125 MHz, CDCl₃): δ 161.8, 159.5, 156.3, 152.0, 150.7, 148.2, 147.7, 144.2, 138.8, 135.1, 132.4, 129.2, 127.6, 124.2, 123.2, 122.9, 121.8, 120.9, 119.5, 118.6, 116.5, 115.2, 115.1, 106.7, 106.4, 56.1, 32.6, 19.9, 8.5 ppm. HRMS (ESI): *m/z* [M + H]⁺ calcd for C₄₀H₃₄N₃O 572.2696, found 572.2709.

Synthesis of 1,3-Bis(dicyanomethylene)indane (I). A solution of indane-1,3-dione (2.4 g, 16 mmol), malononitrile (2.7 g, 41 mmol), and ammonium acetate (1.25 g, 16 mmol) dissolved in absolute ethanol (30 mL) was heated at reflux for 30 min. After the mixture was cooled to room temperature, water (25 mL) was added and the solution acidified with concentrated hydrochloric acid. The brown precipitate was filtered off and washed with water. Recrystallization from glacial acetic acid afforded I as a yellow-brown solid. Yield: 41% (1.6 g). Mp: 255–256 °C. ¹H NMR (500 MHz, CDCl₃): δ 8.67–8.64 (m, 2H), 7.94–7.90 (m, 2H), 4.30 (s, 2H). ¹³C NMR (125 MHz, CDCl₃): δ 165.4, 140.7, 136.4, 127.1, 111.9, 111.7, 79.4, 42.0 ppm. Anal. Calcd for C₁₅H₆N₄ (242.23): C, 74.37; H, 2.50; N, 23.13. Found: C, 74.18; H, 2.46; N, 23.28.

Synthesis of 2-[1,3-Bis(dicyanomethylidene)indan-2-ylidene-nemethyl]-7-(*N,N*-diphenylamino)-9,9-diethylfluorene (5). 7-(Diphenylamino)-9,9-diethylfluorene-2-carbaldehyde (0.56 g, 1.35 mmol) was added to a solution of I (0.3 g, 1.23 mmol) in acetic anhydride (10 mL) at 70 °C with vigorous stirring. The mixture was heated at 70–80 °C for 3 h and cooled. The precipitated solid was filtered off, washed with a small amount of acetic anhydride, and recrystallized from the same solvent, affording dark blue crystals. Yield: 89% (0.70 g). Mp: 291–292 °C. ¹H NMR (500 MHz, CDCl₃): δ 8.77 (s, 1H), 8.7 (d, *J* = 6.3 Hz, 1H), 8.61 (d, *J* = 6.6 Hz, 1H), 7.87 (m, 2H), 7.73 (d, *J* = 6 Hz, 1H), 7.62 (d, *J* = 8.1 Hz, 1H), 7.53 (d, *J* = 8.1 Hz, 1H), 7.40 (s, 1H), 7.32–7.25 (m, 4H), 7.16–7.02 (m, 8H), 1.98–1.87 (m, 4H), 0.42 (t, *J* = 14.7 Hz, 6H). ¹³C NMR (125 MHz, CDCl₃): δ 161.4, 160.4, 152.8, 151.5, 149.4, 147.5, 147.0, 146.0, 138.1, 136.7, 135.0, 134.8, 134.1, 131.4, 130.0, 129.3, 126.2, 125.4, 124.7, 124.4, 123.4, 122.6, 121.9, 120.2, 117.5, 113.3, 113.1, 112.9, 112.2, 71.9, 56.4, 32.6, 8.4 ppm. Anal. Calcd for C₄₅H₃₁N₅ (641.2679): C, 84.22; H, 4.87; N, 10.91. Found: C, 84.09; H, 4.90; N, 11.10. HRMS (ESI-TOF): *m/z* [M + H]⁺ calcd for C₄₅H₃₂N₅ 642.2652, found 642.2630.

Synthesis of (E)-3-(2-(Diphenylamino)-9,9-diethyl-9*H*-fluoren-7-yl)-1-(thiophen-2-yl)prop-2-en-1-one (6). Thiophene-2-carbaldehyde (0.07 g, 0.69 mmol) was added to the solution of KOH (0.04 g, 0.828 mmol) in 5/1 MeOH/H₂O (10 mL). After dissolution, 1-(2-(diphenylamino)-9,9-diethyl-9*H*-fluoren-7-yl)-ethanone (0.30 g, 0.69 mmol) was added to the mixture and stirred for 48 h at reflux. The solid product that precipitated was filtered, washed with hexane, and dried. Recrystallization in hexane provided a yellow solid. Yield: 70% (0.25 g). Mp: 166–167 °C. ¹H NMR (500 MHz, CDCl₃): δ 8.02 (d, *J* = 8 Hz, 1H), 7.97 (d, *J* = 3 Hz, 1H), 7.70 (d, *J* = 8 Hz, 1H), 7.63 (d, *J* = 8.5 Hz, 1H), 7.45 (s, 1H); 7.43 (d, *J* = 6 Hz, 1H), 7.38 (d, *J* = 3 Hz, 1H), 7.29 (bt, *J* = 8 Hz, 5H), 7.14–7.09 (m, 5H); 7.06 (bt, *J* = 8.5 Hz, 3H), 2.05 (m, 2H), 1.93 (m, 2H), 0.36 (t, *J* = 14.5 Hz, 6H). ¹³C NMR (125 MHz, CDCl₃): δ 189.3, 152.7, 150.2, 148.5, 147.7, 146.3, 140.6, 136.6, 135.9, 134.8, 132.0, 131.6, 129.4, 129.0, 128.7, 128.3, 128.2, 124.5, 124.0, 123.2, 122.7, 121.5, 121.2, 120.9, 118.7, 118.2, 56.3, 32.5, 8.5 ppm. HRMS (ESI-TOF): *m/z* [M + H]⁺ calcd for C₃₆H₃₂NOS 526.2199, found 526.2193.

Synthesis of (E)-3-(7-(Diphenylamino)-9,9-diethyl-9*H*-fluoren-2-yl)-1-(thiophen-2-yl)prop-2-en-1-one (7). 1-(Thiophen-2-yl)ethanone (0.046 g, 0.37 mmol) was added to a solution of KOH (0.020 g, 0.37 mmol) in MeOH/H₂O 5/1 (10 mL). After dissolution, 7-(diphenylamino)-9,9-diethylfluorene-2-carbaldehyde (0.15 g, 0.37 mmol) was added to the mixture, and this mixture was stirred for 48 h at reflux. The solid product that precipitated was filtered, washed with hexane, and dried. Purification was carried out by column chromatography (silica gel, hexanes/ethyl acetate 4/1). A yellow solid was obtained. Yield: 80% (0.15 g). Mp: 231–232 °C. ¹H NMR (500 MHz, CDCl₃): δ 7.95 (d, *J* = 15.5 Hz, 1H), 7.91 (dd, *J* = 4 Hz, 1H), 7.68 (dd, *J* = 5 Hz, 1H), 7.64–7.60 (m, 2H), 7.58 (d, *J* = 8.5 Hz, 1H), 7.54 (s, 1H), 7.46 (d, *J* = 16 Hz, 1H), 7.28–7.24 (m, 4H), 7.20 (t, *J* = 8.5 Hz, 1H), 7.13–7.09 (m, 5H), 7.04–7.01 (m, 3H), 2.02–1.88 (m, 4H), 0.38 (t, *J* = 15 Hz, 6H). ¹³C NMR (125 MHz, CDCl₃): δ 182.0, 152.1, 150.57, 148.1, 147.8, 145.8, 144.9, 144.3, 135.3, 133.5, 132.6, 131.5, 129.2, 128.3, 128.1, 124.1, 123.2, 122.8, 122.6, 120.9, 120.1, 119.4, 118.7, 56.1, 32.6, 8.5 ppm. HRMS (ESI-TOF): *m/z* [M + H]⁺ calcd for C₃₆H₃₂NOS 526.2199, found 526.2195.

Linear Spectral Measurements. Linear photophysical properties of all materials were investigated at room temperature in spectroscopic cyclohexane and chloroform. Steady-state absorption spectra were obtained by a UV–visible spectrophotometer in 10 mm path length quartz cuvettes with dye concentrations $1.5 \times 10^{-5} \text{ M} \leq C \leq 3 \times 10^{-5} \text{ M}$. The steady-state fluorescence, excitation, and excitation anisotropy spectra were measured with a spectrofluorimeter in 10 mm spectrofluorometric quartz cuvettes, with dye concentrations $\sim (1-1.5) \times 10^{-6} \text{ M}$. The values of fluorescence quantum yield Φ were determined relative to 9,10-diphenylanthracene in cyclohexane and Rhodamine 6G as standards ($\Phi \approx 0.95$).³⁵

Lifetime Measurements. Lifetime measurements were performed by using a Ti:sapphire laser system (pulse duration $\sim 200 \text{ fs}$ /pulse (fwhm) and 76 MHz repetition rate) coupled with a second harmonic generator (tuning range 350–440 nm). A broad band-pass filter (DS500/200) was placed in front of an avalanche photodiode (APD) detector. Data acquisition was conducted on a time-correlated single photon counting system. The optical densities of all the investigated solutions did not exceed 0.12 at the excitation wavelengths to avoid reabsorption in 10 mm path length quartz cuvettes at room temperature.

Two-Photon Absorption (2PA) Measurements. The 2PA spectra of compounds 1–5 and 7 were measured over a broad spectral region by open aperture Z-scan³⁹ and relative 2PF methods⁴⁰ with Rhodamine B in methanol as a standard.⁴¹ Two-photon induced fluorescence spectra were obtained with a spectrofluorimeter coupled with a regenerative amplified laser system that pumped optical parametric generator/amplifiers generating $\sim 140 \text{ fs}$ output pulses (fwhm) with a repetition rate of 1 kHz. The quadratic dependence of 2PF intensity on the excitation power was verified for every excitation wavelength, λ_{ex} . The same laser system was used for open aperture Z-scan measurements. A comprehensive description of this experimental methodology was previously reported.^{42,43}

X-ray and Computational Methodology. The X-ray diffraction experiments for **1**, **2**, and **6** were carried out with a diffractometer, using Mo K α radiation ($\lambda = 0.71073 \text{ \AA}$) at 100 K. The raw data frames were integrated with the SAINT+ program using a narrow-frame algorithm.⁴⁴ Absorption corrections were applied using the semi-empirical method of the SADABS program.⁴⁵ The structures were solved by direct methods and refined using the Bruker SHELXTL programs suite⁴⁶ by full-matrix least-squares methods on F^2 with SHELXL-97 in an anisotropic approximation for all non-hydrogen atoms. In **1**, the C(31), C(32), N(1), and N(2) atoms of the dicyanovinyl group were disordered over two positions with partial occupancies of 0.64(5) and 0.36(5). All H atoms were placed in idealized positions and refined with constrained C–H distances and $U_{\text{iso}}(\text{H})$ values set to be $1.2U_{\text{eq}}$ or $1.5U_{\text{eq}}$ (for the methyl group) of the attached C atom. Crystallographic data for all structures have been deposited with the Cambridge Crystallographic Data Centre as supplementary publication numbers CCDC 831506–831508. Copies of the data can be obtained, free of charge, on application to the CCDC, 12 Union Road, Cambridge CB2 1EZ, U.K. (fax, +44-(0)1223-336033; e-mail, deposit@ccdc.cam.ac.uk).

All calculations were carried out using the Gaussian09 program.⁴⁷ Starting from crystallographic data (if available), geometry optimizations of molecules **1**–**7** were performed at the B3LYP/6-311G** level^{48–50} for all atoms without any symmetry restriction. The first seven singlet excited states were obtained using time-dependent DFT calculations for isolated molecules starting from optimized geometries at the M06/6-311++G** level of theory.⁵¹ Transition densities associated with the electronic excitations are represented via the natural transition orbital (NTO) formalism.⁵²

■ ASSOCIATED CONTENT

■ Supporting Information

Figures, tables, and CIF files giving ^1H NMR and ^{13}C NMR spectra of **B**, **C**, **1**, **F**, **G**, **2**, **H**, **3**, **4**, **I**, and **5**–**7**, crystallographic structural packing data for **1**, **2**, and **6**, along with X-ray diffraction data (CIF), and computational details, including tables of the optimized geometries of molecules **1**–**7** and ground- and excited-state properties. This material is available free of charge via the Internet at <http://pubs.acs.org>.

■ AUTHOR INFORMATION

Corresponding Author

*E-mail: belfield@ucf.edu. Fax: 407-823-2252. Tel: 407-823-1028.

Notes

The authors declare no competing financial interest.

■ ACKNOWLEDGMENTS

We acknowledge the National Science Foundation (CHE-0832622 and CHE-0840431), the National Institute of Biomedical Imaging and Bioengineering of the National Institutes of Health (1 R15EB008858-01), and the National Academy of Science (PGA-P210877) for support of this work.

■ REFERENCES

- Göppert-Mayer, M. *Ann. Phys.* **1931**, *9*, 273–295.
- He, G. S.; Markowicz, P. P.; Lin, T.-C.; Prasad, P. N. *Nature* **2002**, *415*, 767–770.
- Blanchard-Desce, M. C. R. *Phys.* **2002**, *3*, 439–448.
- Belfield, K. D.; Schafer, K. J.; Liu, Y.; Liu, J.; Ren, X.; Van Stryland, E. W. *J. Phys. Org. Chem.* **2000**, *13*, 837–849.
- Denk, W.; Strickler, J. H.; Webb, W. W. *Science* **1990**, *248*, 73–76.
- Shen, Y.; Jakubczyk, D.; Xu, F.; Swiatkiewicz, J.; Prasad, P. N.; Reinhardt, B. A. *Appl. Phys. Lett.* **2000**, *76*, 1–3.

- Xu, C.; Williams, R. M.; Zipfel, W.; Webb, W. W. *Bioimaging* **1996**, *4*, 198–207.
- Reinhardt, B. A.; Brott, L. L.; Clarkson, S. J.; Dillard, A. G.; Bhatt, J. C.; Kannan, R.; Yuan, L.; He, G. S.; Prasad, P. N. *Chem. Mater.* **1998**, *10*, 1863–1874.
- Baur, J. W.; Alexander, M. D.; Banach, M., Jr.; Denny, L. R.; Reinhardt, B. A.; Vaia, R. A.; Fleitz, P. A.; Kirkpatrick, S. M. *Chem. Mater.* **1999**, *11*, 2899–2906.
- Lee, K.-S.; Lee, J.-H.; Kim, K.-S.; Woo, H.-Y.; Kim, O.-K.; Choi, H.; Cha, M.; He, G. S.; Swiatkiewicz, J.; Prasad, P. N.; Chung, M.-A.; Jung, S.-D. *MCLC S&T, Sect. B: Nonlinear Opt.* **2001**, *27*, 133–137.
- Morel, Y.; Irimia, A.; Najechalski, Y.; Kervella, Y.; Stephan, O.; Baldeck, P. L.; Andraud, C. J. *Chem. Phys.* **2001**, *114*, S391–S396.
- Charlot, M.; Izard, N.; Mongin, O.; Riehl, D.; Blanchard-Desce, M. *Chem. Phys. Lett.* **2006**, *417*, 297–302.
- Reinhardt, B. A. *Photonics Sci. News* **1999**, *4*, 21–34.
- Prasad, P. N.; Bhawalkar, J. D.; Kumar, N. D.; Lal, M. *Macromol. Symp.* **1997**, *118*, 467–472.
- Bhawalkar, J. D.; Kumar, N. D.; Zhao, C. F.; Prasad, P. N. *J. Clin. Laser Med. Surg.* **1997**, *15*, 201–204.
- Verbiest, T.; Houbrechts, S.; Kauranen, M.; Clays, K.; Persoons, A. J. *Mater. Chem.* **1997**, *7*, 2175–2189.
- Le Bozec, H.; Renouard, T. *Eur. J. Inorg. Chem.* **2000**, *2000*, 229–239.
- Wolf, J. J.; Wortmann, R. *Adv. Phys. Org. Chem.* **1999**, *32*, 121–217.
- Long, N. J. *Angew. Chem., Int. Ed. Engl.* **1995**, *34*, 21–38.
- Steybe, F.; Effenberger, F.; Gubler, U.; Bosshard, C.; Günter, P. *Tetrahedron* **1998**, *54*, 8469–8480.
- Albota, M.; Beljonne, D.; Bredas, J.-L.; Ehrlich, J. E.; Fu, J.-Y.; Heikal, A. A.; Hess, S. E.; Kogej, T.; Levin, M. D.; Marder, S. R.; McCord-Maughon, D.; Perry, J. W.; Rockel, H.; Rumi, M.; Subramaniam, G.; Webb, W. W.; Wu, X.-L.; Xu, C. *Science* **1998**, *281*, 1653–1656.
- Marder, S. R.; Gorman, C. B.; Meyers, F.; Perry, J. W.; Bourhill, G.; Bredas, J. L.; Pierce, B. M. *Science* **1994**, *265*, 632–635.
- Oudar, J. L. *J. Chem. Phys.* **1977**, *67*, 446–457.
- Strehmel, B.; Sarker, A. M.; Detert, H. *Chem. Phys. Chem.* **2003**, *4*, 249–259.
- (a) Mignani, G.; Leising, F.; Meyruex, R.; Samson, H. *Tetrahedron Lett.* **1990**, *31*, 4743–4746. (b) Jen, A. K.-Y.; Rao, V. P.; Drost, K. J.; Wong, K. Y.; Cava, M. P. *J. Chem. Soc., Chem. Commun.* **1994**, 2057–2058. (c) Rao, V. P.; Cai, Y. M.; Jen, A. K.-Y. *J. Chem. Soc., Chem. Commun.* **1994**, *14*, 1689–1690.
- Wu, X.; Wu, J.; Liu, Y.; Jen, A.K.-Y. *J. Am. Chem. Soc.* **1999**, *121*, 472–473.
- Belfield, K. D.; Bondar, M. V.; Przhonska, O. V.; Schafer, K. J. *J. Fluoresc.* **2002**, *12*, 449–454.
- Belfield, K. D.; Schafer, K. J.; Mourad, W.; Reinhardt, B. A. *J. Org. Chem.* **2000**, *65*, 4475–4481.
- Belfield, K. D.; Morales, A. R.; Hales, J. M.; Hagan, D. J.; Van Stryland, E. W.; Chapela, V. M.; Percino, J. *Chem. Mater.* **2004**, *16*, 2267–2273.
- Belfield, K. D.; Morales, A. R.; Kang, B.-S.; Hales, J. M.; Hagan, D. J.; Van Stryland, E. W.; Chapela, V. M.; Percino, J. *Chem. Mater.* **2004**, *16*, 4634–4641.
- Morales, A. R.; Belfield, K. D.; Hales, J. M.; Van Stryland, E. W.; Hagan, D. J. *Chem. Mater.* **2006**, *18*, 4972–4980.
- Yao, S.; Belfield, K. D. *J. Org. Chem.* **2005**, *70*, 5126–5132.
- Chiang, C.-L.; Wu, M.-F.; Dai, D.-C.; Wen, Y.-S.; Wang, J.-K.; Chen, C.-T. *Adv. Funct. Mater.* **2005**, *15*, 231–238.
- Bello, K. A.; Cheng, L.; Griffiths, J. J. *Chem. Soc., Perkin Trans 2* **1987**, *6*, 815–818.
- Lakowicz, J. R. *Principles of Fluorescence Spectroscopy*; Kluwer Academic/Plenum: New York, 1999; Vol. 648, pp 52–53, 298–300.
- Rebane, A.; Drobizhev, M.; Makarov, N. S.; Beuerman, E.; Haley, J. E.; Krein, D. M.; Burke, A. R.; Flikkema, J. L.; Cooper, T. M. *J. Chem. Phys. A* **2011**, *115*, 4255–4262.
- http://spie.org/x648.html?product_id=796745.

- (38) Kannan, R.; He, G. S.; Yuan, L.; Xu, F.; Prasad, P. N.; Dombroskie, A. G.; Reinhardt, B. A.; Baur, J. W.; Vaia, R. A.; Tan, L.-S. *Chem. Mater.* **2001**, *13*, 1896–1904.
- (39) Sheik-Bahae, M.; Said, A. A.; Wei, T. H.; Hagan, D. J.; Van Stryland, E. W. *IEEE J. Quantum Elect.* **1990**, *26*, 760–769.
- (40) Xu, C.; Webb, W. W. *J. Opt. Soc. Am. B* **1996**, *13*, 481–491.
- (41) Makarov, N. S.; Drobizhev, M.; Rebane, A. *Opt. Express* **2008**, *16*, 4029–4047.
- (42) Fu, J.; Padilha, L. A.; Hagan, D. J.; Van Stryland, E. W.; Przhonska, O. V.; Bondar, M. V.; Slominsky, Y. L.; Kachkovski, A. D. *J. Opt. Soc. Am. B* **2007**, *24*, 67–76.
- (43) Padilha, L. A.; Webster, S.; Przhonska, O. V.; Hu, H. H.; Peceli, D.; Rosch, J. L.; Bondar, M. V.; Gerasov, A. O.; Kovtun, Y. P.; Shandura, M. P.; Kachkovski, A. D.; Hagan, D. J.; Van Stryland, E. W. *J. Mater. Chem.* **2009**, *19*, 7503–7513.
- (44) SAINT+, Version 6.2a; Bruker Analytical X-ray System, Inc., Madison, WI, 2001.
- (45) SADABS; Bruker Analytical X-ray System, Inc., Madison, WI, 1999.
- (46) SHELXTL, Version 6.10; Bruker Analytical X-ray System, Inc., Madison, WI, 1997.
- (47) Frisch, M. J.; Trucks, G. W.; Schlegel, H. B.; Scuseria, G. E.; Robb, M. A.; Cheeseman, J. R.; Scalmani, G.; Barone, V.; Mennucci, B.; Petersson, G. A.; Nakatsuji, H.; Caricato, M.; Li, X.; Hratchian, H. P.; Izmaylov, A. F.; Bloino, J.; Zheng, G.; Sonnenberg, M.; Hada, M.; Ehara, K.; Toyota, R.; Fukuda, J.; Hasegawa, M.; Ishida, T.; Nakajima, Honda, J. L. Y.; Kitao, O.; Nakai, H.; Vreven, T.; Montgomery, J. A., Jr.; Peralta, J. E.; Ogliaro, F.; Bearpark, M.; Heyd, J. J.; Brothers, E.; Kudin, K. N.; Staroverov, V. N.; Kobayashi, R.; Normand, J.; Raghavachari, K.; Rendell, A.; Burant, J. C.; Iyengar, S. S.; Tomasi, J.; Cossi, M.; Rega, N.; Millam, J. M.; Klene, M.; Knox, J. E.; Cross, J. B.; Bakken, V.; Adamo, C.; Jaramillo, J.; Gomperts, R.; Stratmann, R. E.; Yazyev, O.; Austin, A. J.; Cammi, R.; Pomelli, C.; Ochterski, J. W.; Martin, R. L.; Morokuma, K.; Zakrzewski, V. G.; Voth, G. A.; Salvador, P.; Dannenberg, J. J.; Dapprich, S.; Daniels, A. D.; Farkas, O.; Foresman, J. B.; Ortiz, J. V.; Cioslowski, J.; Fox, D. J. *Gaussian 09, Revision A.02*; Gaussian, Inc., Wallingford, CT, 2009.
- (48) Becke, A. D. *J. Chem. Phys.* **1993**, *98*, 5648–5652.
- (49) Lee, C.; Yang, W.; Parr, R. G. *Phys. Rev. B* **1988**, *37*, 785–789.
- (50) Vosko, S. H.; Wilk, L.; Nusair, M. *Can. J. Phys.* **1980**, *58*, 1200–1211.
- (51) Zhao, Y.; Truhlar, D. G. *Theor. Chem. Acc.* **2008**, *120*, 215–241.
- (52) Martin, R. L. *J. Chem. Phys.* **2003**, *118*, 4775–4777.